Two-Stage Aggregate Formation via Streams in Myxobacteria

M. S. Alber,[1] M. A. Kiskowski,[1] and Y. Jiang[2]

[1]*Mathematics and Physics Departments, University of Notre Dame, Notre Dame, Indiana 46556, USA*
[2]*Theoretical Division, Los Alamos National Laboratory, Los Alamos, New Mexico 87545, USA*

(Received 20 November 2003; published 4 August 2004)

In response to adverse conditions, myxobacteria form aggregates that develop into fruiting bodies. We model myxobacteria aggregation with a lattice cell model based entirely on short-range (nonchemotactic) cell-cell interactions. Local rules result in a two-stage process of aggregation mediated by transient streams. Aggregates resemble those observed in experiment and are stable against even very large perturbations. Noise in individual cell behavior increases the effects of streams and results in larger, more stable aggregates.

DOI: 10.1103/PhysRevLett.93.068102 PACS numbers: 87.18.Ed, 05.40.Ca, 05.65.+b, 87.18.Hf

Introduction.—Fruiting body formation in bacteria occurs in response to adverse conditions [1] and is critical for species survival. When starved, myxobacteria undergo a process of alignment, rippling, streaming, and aggregation that culminates in a three-dimensional fruiting body (Fig. 1). This complex morphogenesis must be robust despite internal and external noise.

Canonically, models for bacteria (e.g., *E. Coli* [2,3] and *B. subtilis* [4,5]) and amoebae (e.g., *D. discoideum* [5,6]) aggregation have been based on chemotaxis, a long range cell interaction that shares many features of chemical reaction-diffusion dynamics. Initialization of chemotactic signals plays an important role in the initial position of aggregates [2,7] and subsequent signaling biases cell motion towards developing aggregates [2]. Cells following the maximal chemical gradient navigate towards aggregates that are large and near. In myxobacteria there are no chemotactic cues [8,9], yet cells travel large distances to enter an aggregate [10]. Models based on cell collisions have reproduced myxobacteria rippling patterns [11,12]. Recently an earlier model for rippling has been extended to include aggregation [13]. Our model is complementary to this continuum model, and focuses on aggregation without rippling.

During aggregation, myxobacteria cells are elongated with a 7:1 length to width ratio (typically 2 to 12 by 0.7 to 1.2 μm [14]). They move on surfaces by gliding along their long axis [15]. Fruiting body development is controlled by the *C*-signal morphogen, which is exchanged by cell-cell contact at cell poles [16]. Different levels of *C* signal, encoded by the csgA gene, induce the different stages of fruiting body formation [17,18]. Each time a cell receives the *C* signal it increases expression of csgA [17,19]. Aggregates are composed of 10^4 to 10^6 cells [14].

Several models have been proposed to explain myxobacteria aggregation [9]. One describes aggregation by cells following the slime trails deposited by other cells, but finds these aggregates unstable without additional chemotaxis [20]. Another suggests that cells form streams by sequential end-to-end contacts due to *C* signaling, which coalesce or spiral in on themselves; but these aggregates remain unstable as long as cells are motile [19]. However, experiments show that cells move faster within aggregates [21].

We report a new mechanism for aggregate formation in myxobacteria: *two-stage aggregation via streams*. This mechanism, based entirely on local cell-cell interactions, accounts for both initiation and growth of large stable aggregates.

Model.—Our model is based on local rules by which cells turn preferentially in directions that increase their level of *C* signaling. On a hexagonal lattice with periodic boundary conditions, unit velocities (or *channels*) are allowed in each of the six directions. Cells are initially randomly distributed with a cell density 10, where cell density is the sum of all cell areas divided by total lattice area. We model identical rod-shaped cells as 3×21 rectangles and assume a cell size of 1×7 μm. The cell is represented as follows: (1) a single occupied lattice node corresponds to the cell's center in the xy plane, (2) an occupied channel at this node designates the cell's velocity, and (3) a local neighborhood defines the size and shape of the cell. An exclusion rule demands that there may be only one cell center per channel per node. This cell representation is computationally efficient, yet approximates aggregates more closely than using pointlike cells.

Two *C* signal exchange neighborhoods are at the poles of each cell, consisting of 7 nodes each. *C* signaling occurs when the *C*-signaling nodes at the head of a cell overlap with the *C*-signaling nodes at the tail of another

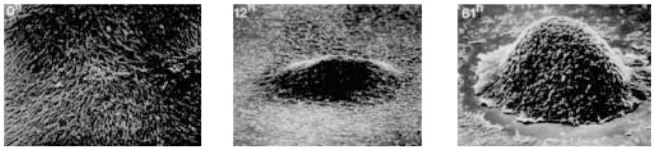

FIG. 1. Snapshots during the fruiting body formation of *M. xanthus* at 0, 12, and 61 h (from [25] with permission).

cell, the value ranging between 0 and 7. At each time step, the cell may turn 60° or stay in its current direction, with a preference of the direction with maximum C-signaling value. The probability for a given cell to turn from orientation θ to θ' is $P = \frac{e^{\beta C(\theta')}}{Z(\theta)}$, if $\theta' = (\theta, \theta + \frac{\pi}{6}, \theta - \frac{\pi}{6})$ and $P = 0$ otherwise, where $C(\theta)$ is the C-signaling value, the normalization factor $Z(\theta)$ is $e^{\beta C(\theta)} + e^{\beta C(\theta+\frac{\pi}{6})} + e^{\beta C(\theta-\frac{\pi}{6})}$, with $\beta = 0.5$. This rule causes cell alignment, a simplification of the hypothesis that alignment and C signaling reinforce each other [17,19].

Simulation results.—Cells aggregate in two distinctive stages in our simulations. During the first stage, initially randomly distributed cells condense into small stationary aggregates [Fig. 2(a)], which grow and absorb immediately surrounding cells. Next, some adjacent stationary aggregates merge and form long, thin streams, which extend and shrink or interact with other aggregates [Fig. 2(b)]. These streams eventually disappear, leaving behind a new set of larger, denser stationary aggregates that are stable over time [Fig. 2(c)]. Figure 2(d) shows an experimental figure in which two aggregates are interacting via a stream.

Cells in a typical aggregate form an annulus of aligned cells tangent to a hollow center [Fig. 3(a)]. Within streams, cells move head to tail with each other in either direction along the stream [see Fig. 3(b)]. Figure 3(c) shows the details of the stream forming from two interacting aggregates. Initial aggregates crowd as they grow. When the distance between aggregates is less than one cell length, they begin exchanging cells and reorganizing

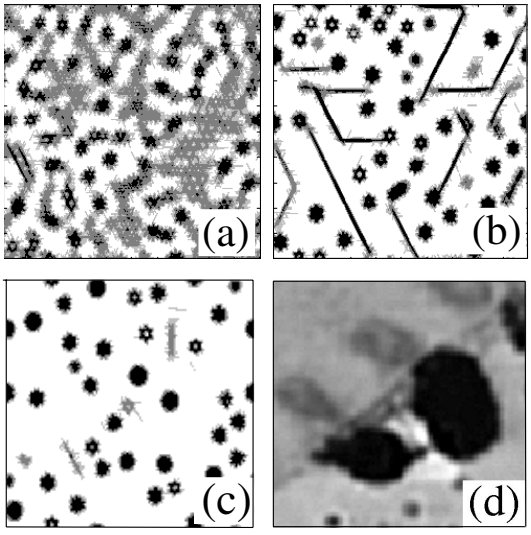

FIG. 2. Aggregation stages on a 500×500 lattice, corresponding to an area of 2.8 cm^2. Local cell density after (a) 200, (b) 900, and (c) 25 000 time steps, with average cell density 10. The darker shade of gray corresponds to a higher cell density. (d) The formation of a stream between two experimental *M. xanthus* aggregates (from [26] with permission).

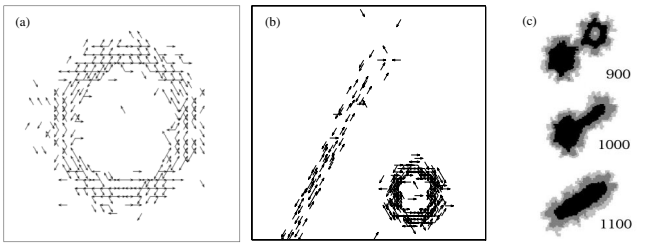

FIG. 3. Directions of cell centers within (a) a typical annular aggregate on a 30×30 lattice subsection and (b) a typical stream adjacent to an aggregate on a 100×100 lattice subsection. (c) Stream formation from two adjacent aggregates at 900, 1000, and 1100 time steps.

into a stream. In contrast to stationary aggregates, cells travel long distances in streams.

Role of noise.—We measured the areas and densities of every stationary aggregate that appeared over the course of two simulations. These aggregates fall within a narrow region in the area-density phase diagram shown in Fig. 4(a), which we call an attractor region. We now analyze the stability of this attractor region with respect to two kinds of noise: (1) external noise, which is noise from the random initial condition and from our perturbations; (2) internal noise, which originates from the stochastic nature of the cell's turning process.

1. External noise: Simulations for different random initial conditions show that the standard deviation of local cell density increases with similar slopes and to similar levels (data not shown), indicating that aggregation is not sensitive to noise from the initial conditions.

Next we perturb a stable aggregate in two ways. First, we study an adiabatic perturbation. As cells are slowly added to an initially small aggregate, the aggregate increases in area and density while remaining within the attractor region [Fig. 4(b)]. The oscillation of the path corresponds to "pulsing" of an aggregate [22]. Second, we perform a nonadiabatic perturbation by placing two duplicate aggregates next to each other, which creates a new aggregate with double the initial area and the same density. Over 600 time steps, this aggregate reorganizes

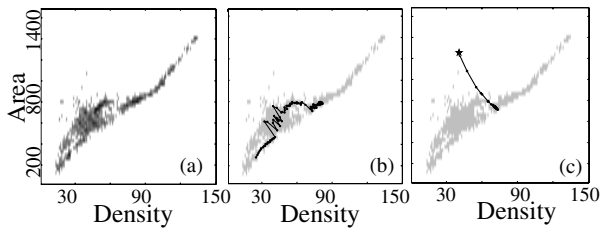

FIG. 4. Area-density phase diagram for (a) 186 stationary aggregates identified within two simulations over 25 000 time steps, (b) an initially small aggregate to which cells are slowly added over 1000 time steps, and (c) an artificially constructed aggregate (star) over 600 time steps. Relaxation of perturbation data in (b) and (c) are plotted on top of (a).

so that it has an area and density within the stable region [Fig. 4(c)]. These responses to both kinds of perturbations suggest that the attractor region is stable.

The area-density phase diagram, in addition to prescribing the region of stable aggregates, helps our understanding of the formation and stability of streams. When two stationary aggregates interact, the newly formed aggregate lies off the attractor region. Large aggregates fuse and quickly form a new stable aggregate as in Fig. 4(c). Small aggregates, because they have lower cell density and lower *C*-signaling levels, and thus a longer transient stage, are more likely to form a stream when they fuse. Cells at the end of streams diffuse without any preferred direction. Although randomly diffusing cells often find their way back into the stream, some cells escape from the stream. Over time, the stream shortens as it gradually loses cells. Once the stream is quite short, it reorganizes into an aggregate after a brief disordered transient.

2. Internal noise: To evaluate the role of internal noise, we devise a corresponding deterministic model. Instead of a stochastic process for cell turning, we use the following function to determine the cell orientation for the next step:

$$\begin{aligned} f_i(r, k+1) = {} & f_i(r - c_i^{\ominus}, k)\Omega(r - c_i^{\ominus}, k, c_i) \\ & + f_i(r - c_i^{\oplus}, k)\Omega(r - c_i^{\oplus}, k, c_i) \\ & + f_i(r - c_i, k)\Omega(r, k, c_i), \end{aligned}$$

where f is the cell density distribution function, and c_i, $c_i^{\ominus}$, and $c_i^{\oplus}$ represent vectors in the ith direction, clockwise from the ith direction, and counterclockwise, respectively. The collision function $\Omega(r, k, i)$ is the cell density distribution function of a cell at the node r turning towards direction i at the kth time step. We drop the exclusion principle so that the local cell density may exceed 1. This function converts our stochastic model into a deterministic model, analogous to the process of changing a stochastic lattice gas model to a deterministic lattice Boltzmann model [23].

This deterministic model evolves similarly to the stochastic model, indicating that the aggregation dynamics are not sensitive to internal noise. The important differences are that in the deterministic model, streams are fewer and smaller, and shorter lived, and that the simulation reaches a steady state much faster. These differences have a critical effect on the way aggregates reorganize. Comparing the size distribution of aggregates in both models [Figs. 5(a) and 5(b)], we see that, with the internal noise, aggregates can reach larger sizes. This is not surprising because noise slows stream contraction so that streams persist longer and span a greater area, enabling more aggregates to interact and form larger, more stable aggregates.

Discussion.—In our simulations, streams redistribute cells within fewer, larger aggregates. This is a new mechanism for large, stable aggregate formation in which aggregates first form at random locations and then reorganize. Cells can span great distances by moving within streams.

The aggregates in our simulations reproduce the unique structures of several myxobacteria fruiting bodies. In *M. xanthus,* the basal region of the fruiting body is a shell of densely packed cells that travel both clockwise and counterclockwise around an inner region only one-third as dense [21,24]. Figure 3(a) shows that typical simulation aggregates have this geometry, and cell tracking shows that cells orbit in both directions. Further, aggregates in our simulation often form in clusters of two or three closed orbits while in *S. erecta,* several fruiting bodies may form in groups and fuse [14].

In experiments, one myxobacteria aggregate has been observed to mysteriously grow as an adjacent aggregate disappears [22]. Our model offers an explanation: a stream may form connecting two adjacent aggregates, and cells migrate from the smaller aggregate to the larger aggregate. Experimentally, these streams may not be visible due to low resolution. Figure 2(d) shows a barely visible stream between two aggregates. Shortly after this stream forms, the two aggregates fuse.

This mechanism suggests several predictions that may be tested experimentally. We predict that the formation of streams and subsequent redistribution of aggregates will be most significant for intermediate initial cell densities. At low density, the initial set of aggregates are too far apart to interact. At high cell density, large, dense aggregates fuse immediately when they interact rather than form a stream. The role of external noise can be experimentally tested by repeating the perturbation experiments we describe in Figs. 4(b) and 4(c). Cells may be slowly added to a small aggregate or quickly added to an aggregate by a large amount to observe the cell reorganization over time. Finally, the role of internal noise can be tested by tuning the level of *C* signaling. For example, *C* signaling can be decreased by diluting a wild-type population with non-*C*-signaling cells (increasing internal

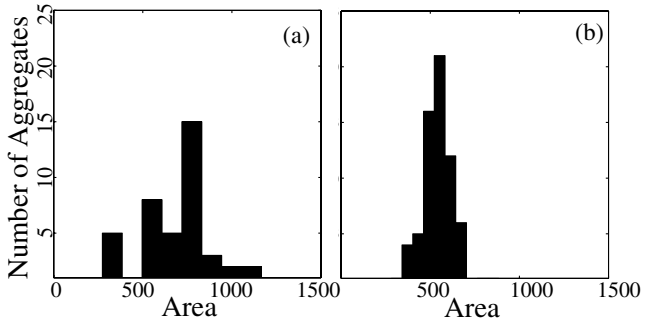

FIG. 5. Final distribution of stationary aggregate areas for (a) a stochastic simulation and (b) the equivalent deterministic simulation.

noise) or individual cell *C*-signaling levels can be increased (decreasing internal noise).

The limited number of directions permitted on a hexagonal lattice results in an overly regular local pattern and limits the size of aggregates in our simulation, since cells capable of turning by 60° at each time step may follow a circular orbit with a small radius of curvature. Our local rules do not prevent cells from stacking very high, which results in smaller aggregates and thinner streams. For example, myxobacteria aggregates range in size from 10 to 1000 μm in diameter, while in our simulations aggregate size is up to 15 μm. Thus our model suggests a mechanism only qualitatively. Additional rules, such as cell jamming, would be required to reproduce more details of aggregate formation.

Summary.—Our lattice cell model is based on simple local rules by which cells align by turning preferentially to make end to end contacts. On average this rule results in cells following the tails of other cells, mimicking the effect of *C* signaling in myxobacteria that drives aggregation. In our simulations, distinct aggregate types form that have different behaviors and roles even though they are composed of identical cells following identical rules. Large, stationary aggregates are stable, while intermediate motile aggregates (streams) can aid in large aggregate formation. An interesting discovery is that the presence of internal noise is required for efficient streaming. It is as if the cells must make short-term mistakes to form unstable transients that ultimately results in more efficient aggregation. Our analysis of streams and noise suggests some new experiments.

We thank Dr. Dale Kaiser, Dr. Stan Maree, and Dr. Guy McNamara for fruitful discussions. M. S. A. is partially supported by Grant No. NSF IBN-0083653. M. A. K. and Y. J. are supported by DOE under Contract No. W-7405-ENG-36. M. A. K. also acknowledges support from CAM and ICSB centers, University of Notre Dame.

[1] E. Ben-Jacob *et al.*, Nature (London) **368**, 46 (1994).
[2] L. Tsimring *et al.*, Phys. Rev. Lett. **75**, 1859 (1995).
[3] M. P. Brenner *et al.*, Biophys. J. **74**, 1677 (1998).
[4] M. Matsushita and H. Fujikawa, Physica (Amsterdam) **168A**, 498 (1990); I. Golding *et al.*, Physica (Amsterdam) **260A**, 510 (1998); A. Komoto *et al.*, J. Theor. Biol. **225**, 91 (2003).
[5] E. Ben-Jacob *et al.*, Adv. Phys. **49**, 395 (2000).
[6] T. Höfer *et al.*, Proc. R. Soc. London B **259**, 249 (1995).
[7] J. Y. Wakano *et al.*, Phys. Rev. Lett. **90**, 258102 (2003).
[8] S. Lobedanz and L. Søgaard-Andersen, Genes Dev. **17**, 2151 (2003).
[9] For a review, see M. Dworkin, Microbiol. Rev. **60**, 70 (1996).
[10] L. Jelsbak and L. Søgaard-Andersen, Curr. Opin. Microbiol. **3**, 637 (2000).
[11] O. Igoshin *et al.*, Proc. Natl. Acad. Sci. U.S.A. **98**, 14913 (2001); F. Lutscher and A. Stevens, J. Nonlinear Sci. **12**, 619 (2002); U. Borner *et al.*, Phys. Rev. Lett. **89**, 078101 (2002).
[12] M. S. Alber *et al.*, Physica (Amsterdam) **191D**, 343 (2004).
[13] O. Igoshin, R. Welch, D. Kaiser, and G. Oster, Proc. Natl. Acad. Sci. U.S.A. **101**, 4256 (2004).
[14] H. Reichenbach, in *Myxobacteria II*, edited by M. Dworkin and D. Kaiser (American Society for Microbiology, Washington, DC, 1993).
[15] R. P. Buchard, Annu. Rev. Microbiol. **35**, 497 (1981).
[16] S. K. Kim and D. Kaiser, Genes Dev. **4**, 896 (1990); Science **249**, 926 (1990).
[17] S. K. Kim and D. Kaiser, J. Bacteriol. **173**, 1722 (1991); S. Li, B. Lee, and L. J. Shimkets, Genes Dev. **6**, 401 (1992).
[18] T. Kruse *et al.*, Mol. Microbiol. **40**, 156 (2001).
[19] L. Jelsbak and L. Søgaard-Andersen, Proc. Natl. Acad. Sci. U.S.A. **99**, 2032 (2002).
[20] A. Stevens, SIAM J. Appl. Math. **61**, 172 (2000).
[21] B. Sager and D. Kaiser, Proc. Natl. Acad. Sci. U.S.A. **90**, 3690 (1993).
[22] D. Kaiser (private communication).
[23] U. Frisch *et al.*, Complex Syst. **1**, 249 (1987).
[24] B. Julien, D. Kaiser, and A. Garza, Proc. Natl. Acad. Sci. U.S.A. **97**, 9098 (2000).
[25] J. M. Kuner and D. Kaiser, J. Bacteriol. **151**, 458 (1982).
[26] D. Kaiser and R. Welch, J. Bacteriol. **186**, 919 (2004).